



Article

A Method for Prediction of Winter Wheat Maturity Date Based on MODIS Time Series and Accumulated Temperature

Fa Zhao ^{1,2,3,4}, Guijun Yang ^{2,4,5,*}, Hao Yang ^{2,4} , Huiling Long ^{2,4}, Weimeng Xu ⁵, Yaohui Zhu ^{2,4} , Yang Meng ^{2,4}, Shaoyu Han ^{2,4} and Miao Liu ^{2,4}

¹ School of Electrical Engineering, Anhui Polytechnic University, Wuhu 241000, China; p18101005@stu.ahu.edu.cn

² Key Laboratory of Quantitative Remote Sensing in Agriculture of Ministry of Agriculture and Rural Affairs, Information Technology Research Center, Beijing Academy of Agriculture and Forestry Sciences, Beijing 100097, China; yangh@nercita.org.cn (H.Y.); longhl@nercita.org.cn (H.L.); yaohui_zhu@bjfu.edu.cn (Y.Z.); mengy@nercita.org.cn (Y.M.); 13598834331@stu.henau.edu.cn (S.H.); 19210010011@stu.xust.edu.cn (M.L.)

³ School of Electronic and Information Engineering, Anhui University, Hefei 230601, China

⁴ National Engineering Research Center for Information Technology in Agriculture, Beijing 100097, China

⁵ College of Geological Engineering and Geomatics, Chang'an University, Xi'an 710054, China; 2019126031@chd.edu.cn

* Correspondence: yanggj@nercita.org.cn

Abstract: Accurate determination of crop phenology is key to field management and decision making. The existing research on phenology based on remote sensing data is mainly phenology monitoring, which cannot realize the prediction of phenology. In this paper, we propose a method to predict the maturity date (MD) of winter wheat based on a combination of phenology monitoring method and accumulated temperature. The method is divided into three steps. First, 2-band Enhanced Vegetation Index (EVI2) time series data were generated using the moderate-resolution imaging spectroradiometer (MODIS) reflectance data at 8-day intervals; then, the time series were reconstructed using polynomial fitting and the heading date (HD) of winter wheat was extracted using the maximum method. Secondly, the average cumulative temperature required for winter wheat to go from HD to MD was calculated based on historical phenological data and meteorological data. Finally, the timing of winter wheat HD and the current year's Meteorological Data were combined to predict winter wheat MD. The method was used to predict the MD of winter wheat in Hebei in 2018 and was validated with data from the phenology station and the Modis Land Cover Dynamics (MCD12Q2) product. The results showed that the coefficient of determination (R^2) for predicting MD using this method was 0.48 and 0.74, the root mean square error (RMSE) was 7.03 and 4.91 days, and Bias was 4.93 and -3.59 days, respectively. In summary, the method is capable of predicting winter wheat MD at the regional scale.

Keywords: prediction; winter wheat; maturity; MODIS; accumulated temperature



Citation: Zhao, F.; Yang, G.; Yang, H.; Long, H.; Xu, W.; Zhu, Y.; Meng, Y.; Han, S.; Liu, M. A Method for Prediction of Winter Wheat Maturity Date Based on MODIS Time Series and Accumulated Temperature. *Agriculture* **2022**, *12*, 945. <https://doi.org/10.3390/agriculture12070945>

Academic Editor: Josef Eitzinger

Received: 9 January 2022

Accepted: 24 June 2022

Published: 29 June 2022

Publisher's Note: MDPI stays neutral with regard to jurisdictional claims in published maps and institutional affiliations.



Copyright: © 2022 by the authors. Licensee MDPI, Basel, Switzerland. This article is an open access article distributed under the terms and conditions of the Creative Commons Attribution (CC BY) license (<https://creativecommons.org/licenses/by/4.0/>).

1. Introduction

As one of the important directions of agricultural development, precision agriculture can greatly improve the yield and quality of crops and reduce variability and input costs [1–3]. Crop phenology is an important indicator in the process of crop growth [4–6]. Accurate acquisition of crop phenology plays a very important role in agricultural production, management, and decision-making and is one of the important elements of precision agriculture [7,8].

The research on crop phenology is mainly focused on crop phenology monitoring. The traditional method of phenology monitoring is to determine the phenology by directly observing the growth and development of crops on the ground, which is a simple and

accurate method. However, this method is time-consuming, labor-intensive, and only suitable for small-scale observation. In recent years, due to the rapid development of remote sensing technology, the use of remote sensing data for crop phenology monitoring has been increasingly applied [9]. Among them, crop phenology monitoring based on time-series remote sensing data is the most widely used [5,8,10–19]. At present, there are two main types of methods for monitoring the weathering period using time-series remote sensing data: one is the threshold method [20–23] and the other is the change detection method [9,24–29].

White et al. combined remotely sensed phenology monitoring with traditional meteorological phenology modeling, proposed the ratio threshold method for the continental ecosystem phenology of the United States, and extracted the vegetation phenology of 56 meteorological stations in the United States from 1990 to 1992 for comparative verification. Jönsson and Eklundh used the period when the normalized difference vegetation index (NDVI) reaches 10% of its maximum annual amplitude as the beginning and end of the vegetation growing season. Vrieling et al. defined the start of the season (SOS) as the point at which NDVI reaches 20% of its maximum annual amplitude and the peak season (PS) as the point at which NDVI reaches 90% of its maximum annual amplitude. In addition, Gan et al. used the relative threshold methods, including relative thresholds of 10%, 20%, or 50% of the vegetation index amplitude, to detect the green-up date (GUD) of winter wheat in the Huanghuaihai winter wheat region of China from 2009 to 2013. Zhang et al. used the extreme points of curvature change as the GUD, MD, decay, and dormancy of vegetation growth based on fitting the moderate-resolution imaging spectroradiometer (MODIS) vegetation index. In addition, Lu et al. determined the SOS of winter wheat in the North China Plain as the time corresponding to the maximum derivative of the NDVI time series curve. Liu et al. [27] used maximum curvature change and maximum change with different curve fitting algorithms to extract the spring green-up date derived from global inventory modeling and mapping studies (GIMMS) and spot vegetation (SPOT-VGT) NDVI of winter wheat cropland in the north China plain. Chu et al. used the maximum curvature method to extract the winter wheat phenological date by determining the green-up, heading, and harvesting phases when the NDVI curvature reaches a local maximum [29].

Crop phenology monitoring based on time-series remote sensing data is based on the extraction of phenology when phenology has already occurred, and more often, we would like to predict crop phenology when it has not yet occurred. At present, there are few researches on crop phenology prediction based on remote sensing time series data. Liu et al. [16] integrated timely available visible infrared imaging radiometer suit (VIIRS) observations and the climatology (expectation and standard deviation) of vegetation phenology from long-term MODIS data to simulate a set of potential temporal trajectories of greenness development at a given time for each pixel. These potential trajectories were then applied to identify spring green leaf development in real time and predict the occurrence of green-up onset, mid-green-up phase, and maturity onset. Zhuo et al. used the leaf area index (LAI) product of MODIS fused to the data assimilation framework of the world food studies (WOFOST) model to calculate the predicted maturity of winter wheat in Henan Province [30].

In this paper, we propose a new phenological date prediction method to predict the maturity date of winter wheat by combining MODIS time-series remote sensing data and meteorological data. First, MODIS 2-band Enhanced Vegetation Index (EVI2) [31] time series data are generated using MODIS reflectance data at 8-day intervals; then, the time series are reconstructed using polynomial fitting and the HD of winter wheat is extracted using the maximum method [25,32,33]. Secondly, the average cumulative temperature required for winter wheat to go from HD to MD was calculated based on historical phenological data and meteorological data. Finally, the timing of winter wheat HD and the current year's meteorological data were combined to predict winter wheat MD.

2. Study Area and Data

2.1. Study Area

The study area is Hebei Province ($36^{\circ}05'–42^{\circ}40' \text{ N}$ and $113^{\circ}27'–119^{\circ}50' \text{ E}$) located in northeastern China (Figure 1). Hebei Province has a complex topography with plains, plateaus, mountains, hills, and lakes interspersed. The plains are mainly located in the southeast, with an area of 8.15×10^4 square meters. The region has a temperate continental monsoon climate with four distinct seasons and abundant precipitation (484.5 mm average annual precipitation), 2303 h of annual sunshine, and a long frost-free period (204 days). The crops in Hebei Province are mainly wheat, corn, cotton, rice, and potatoes. Among them, winter wheat and summer corn are the two crops with the highest replanting rate [34]. Winter wheat is usually sown in early October and comes to maturity for harvest in mid-June.

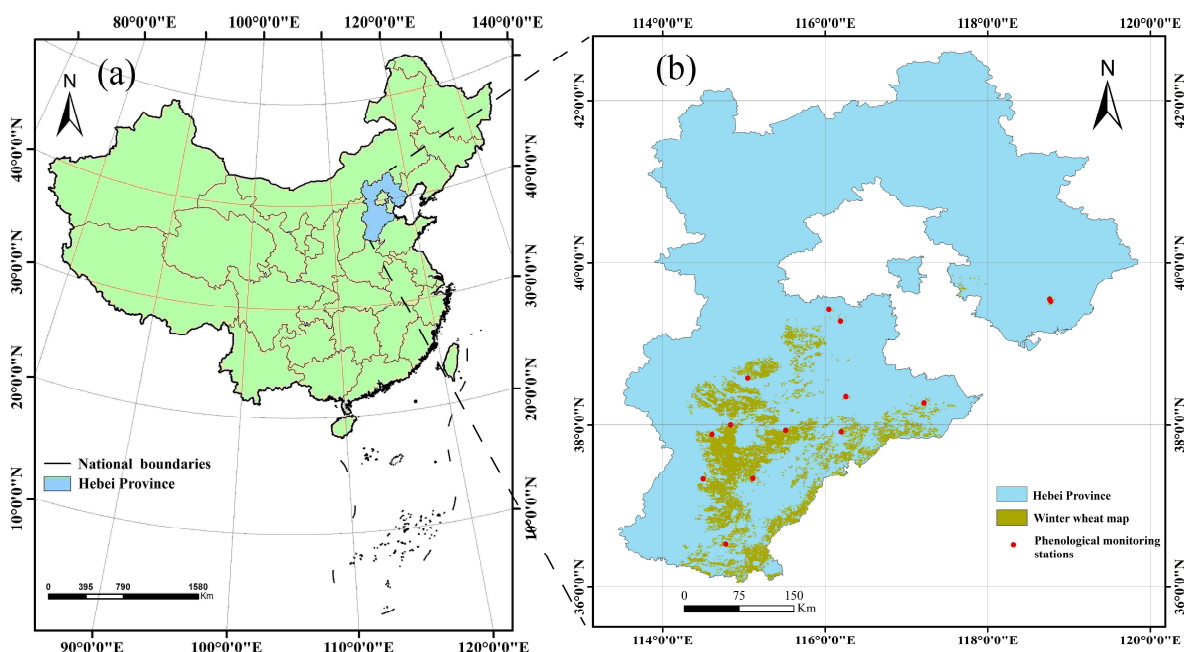


Figure 1. (a) The location of the study area. (b) The winter wheat map and phenological monitoring stations.

In order to obtain the EVI2 time series of winter wheat, we need to know the planting distribution of winter wheat in Hebei Province. In this study, the planting distribution map of winter wheat in 2018 provided by Zhao et al. [35], with a spatial resolution of 500 m, was adopted. In this map, the author uses the time-weighted dynamic time warping (TWDTW) algorithm [36–39] to extract the planting distribution of winter wheat in Hebei province, and the overall classification accuracy is 94.74%. Since the winter wheat in Hebei Province is mainly planted in the plains, the wheat varieties and management methods are roughly the same. In terms of time, it is basically sown in early October and harvested at the end of June the following year. In terms of space, according to the planting area statistics of the Hebei Provincial Bureau of Statistics, the error in the planting area of winter wheat from 2015 to 2018 was within 2%. To sum up, it can be considered that winter wheat planting structure in Hebei Province is relatively stable, and there is no need to draw the map of winter wheat every year [23].

2.2. Data

The data used in this study include the following: remote sensing data, meteorological data, MODIS land cover dynamics product (MCD12Q2) product data, and phenological monitoring station data. Among them, remote sensing data, meteorological data, and MCD12Q2 product data are downloaded through the Google Earth Engine (GEE) plat-

form (<https://earthengine.google.com>, accessed on 20 October 2021), which is capable of accessing information from satellite images and other earth observation databases and provides sufficient computing power to process these data [40]. The phenological monitoring station data were obtained from the meteorological data sharing service system of China (<http://data.cma.cn>, accessed on 10 October 2021). This dataset contains field records of crop growth and development since September 1991. The data include crop varieties, names and dates of crop development stages, etc. These data are described in the following sections.

2.2.1. Remote Sensing Data and Processing

MODIS surface reflectance products provide estimates of surface spectral reflectance measured at ground level, with geometric, radiometric, and atmospheric corrections applied to the lower level data products to produce higher-order level 2 and level 3 products. The data used in this study, MOD09A1, are a Level 3 product, which provides bands 1–7 with a spatial resolution of 500 m in an 8-day period. In order to obtain MODIS EVI2 [41,42] time series data for winter wheat, we carried out the following processing:

- (1) MOD09A1 data were downloaded for the Hebei Province region of China for the period from 1 January 2015 to 25 May 2018.
- (2) The MODIS EVI2 time series for the entire Hebei Province region was obtained by calculating the EVI2 equation.

$$EVI2 = 2.5 \times \frac{\rho_{NIR} - \rho_{RED}}{\rho_{NIR} + 2.4\rho_{RED} + 1} \quad (1)$$

where ρ_{NIR} and ρ_{RED} are the surface reflectance values of the red band (0.62–0.67 μm) and the near-infrared band (0.84–0.87 μm) of the Modis sensor, respectively.

- (3) The start and end dates of the EVI2 time series for winter wheat were determined for each year.

In Hebei Province, the crops are mainly winter wheat and corn in rotation [34]; so, we needed to remove the influence of EVI2 during corn growth. The growth cycle of winter wheat is generally planted in October of the previous year, returned to green jointing the following spring, and harvested in June. Start planting corn after the winter wheat is harvested. Therefore, in order to predict the EVI2 of winter wheat, in this study, we chose 1 January to 30 June of the following year as the growth cycle of winter wheat for monitoring and prediction. During this time period, the main phenological phases of winter wheat are included.

2.2.2. Meteorological Data

The European Centre for Medium-Range Weather Forecasts (ECMWF) dataset is a global atmospheric reanalysis dataset that has been in use since 1979 and is still used today. The ECMWF medium-term reanalysis (ERA-Interim) system provides a large amount of information for weather prediction models. In this study, considering the actual growth condition of winter wheat in Hebei, winter wheat draws in April–May and matures in June. We collected temperature grid data from 1 April to 30 June from 2015 to 2018, with a total of 364 gridded image data points. It has a spatial resolution of 0.1 degrees, which is resampled to raster data with a spatial resolution of 500 m to obtain the same spatial resolution as the MODIS EVI2 data.

2.2.3. Phenological Monitoring Station Data and MCD12Q2 Product Data

Data from 14 phenological monitoring stations in Hebei Province were used (Figure 1b), each of which recorded the HD and MD. The ground HD was recorded by observers when more than half of the top of the ear (excluding the awns) was exposed from the leaf sheath in a wheat field near the station; the ground MD was recorded by observers when the endosperm of more than 50% of grains was waxy, and the ear and the mode under the ear

had turned yellow in a wheat field near the station. We collected a total of 212 phenological data points for winter wheat from 2015 to 2018, where data from 2015 and 2017 were used to construct a cumulative temperature model. The 2018 phenological data were used for extraction as well as validation of prediction results.

MCD12Q2 provides global phenology maps at 500 m and annual time steps since 2001. The product contains 25 reference tables recording the timing of phenology, such as onset of greenness increase, peak greenness, senescence, and dormancy. In this study, we used the 2018 Hebei MCD12Q2 product and extracted the bands Peak_1, defined as the date when EVI2 reached the segment maximum, and Dormancy_1, defined as the date when EVI2 last crossed 15% of the segment EVI2 amplitude. We used Peak_1 as the HD and Dormancy_1 as MD [43].

3. Methodology

Based on MODIS EVI2 time series data, meteorological data, phenological monitoring station data, and the winter wheat map, the MD of winter wheat in Hebei Province was predicted based on the estimation of winter wheat HD combined with the cumulative temperature model, including the following steps: (a) the extraction of winter wheat HD; (b) the calculation of average accumulated effective temperature (AET_{ave}) from HD to MD; (c) the prediction of MD (Figure 2).

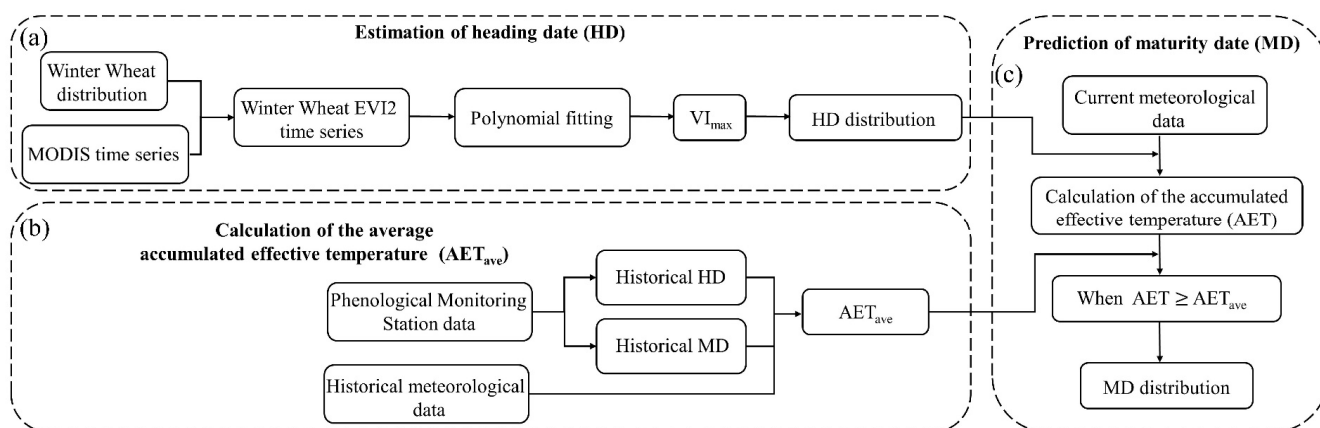


Figure 2. Workflow of the prediction of maturity date (MD). (a) Estimation of heading date (HD). (b) Calculation of average accumulated effective temperature (AET_{ave}). (c) Prediction of maturity date (MD).

3.1. Estimation of HD

In this study, the maximum value method [28,29,44,45] was used to estimate the HD of winter wheat. The maximum value method refers to using the date corresponding to the maximum value of vegetation index time series to represent the phenological phase. The main steps are as follows: firstly, the winter wheat EVI2 time series generated by winter wheat distribution and MODIS remote sensing time data were used to simulate the growth and development process of winter wheat. Secondly, the vegetation index curve was fitted by fitting method and reconstructed into daily EVI2 time series. Common fitting methods include SG filtering, asymmetric Gaussian fitting, double logistic fitting, and polynomial fitting. In this study, six-order polynomial function fitting was used in phenological extraction [46–48]. Finally, the date corresponding to the maximum value of EVI2 time series reconstructed by fitting was extracted as the HD of winter wheat.

3.2. Calculation of Average Accumulated Effective Temperature (AET_{ave})

The crop development dataset from 2015 to 2018 during the fertility period of winter wheat in Hebei and the dataset of daily values of Chinese ground climate data were selected for modeling. The accumulated effective temperature (AET) from HD to MD was calculated for each meteorological station by combining the HD and MD of winter wheat provided by

the meteorological stations, and finally, the AET was averaged over three years to obtain the average accumulated effective temperature (AETave) from HD to MD.

The effective temperature (ET) and AET are calculated as shown in Equations (2) and (3), respectively.

$$ET_i = \begin{cases} T_i - T_b, & T_i \geq T_b \\ 0, & T_i < T_b \end{cases} \quad (2)$$

$$AET = \sum_{i=Start_Day}^{End_day} ET_i \quad (3)$$

where T_i represents the mean air temperature of the i th day and T_b represents the baseline temperature, which was set to 0 °C [49]. ET_i represents the effective temperature of the i th day; $Start_Day$ and End_day represent the starting and ending days for calculating the accumulated effective temperature, respectively.

3.3. Prediction of MD

Combining the extracted HD and meteorological data of 2018, the MD of winter wheat can be predicted. The specific process is that the HD is recorded first; then, the gradual accumulation of effective temperature is carried out from the HD, and the MD of winter wheat is considered to be reached when the accumulated effective temperature (AET) reaches the AETave calculated above. The predicted MD is calculated as shown in Equation (4).

$$MD = HD + Days, \text{ when } AET = \sum_{i=HD}^{HD+Days} ET_i \geq AET_{ave} \quad (4)$$

where MD represents the maturity date; HD represents the heading date; and Days represents the cumulative temperature of winter wheat from HD, after the number of days, to reach the AETave.

3.4. Accuracy Validation

In this paper, we used two datasets to verify the extraction results of HD and prediction results of MD due to the large difference in spatial scale between the phenological monitoring station data and the remote sensing data: one is the phenological monitoring station dataset, the other is MCD12Q2 product dataset. The spatial resolution of remote sensing data is 500 m, while the phenological monitoring station data are point data, which will lead to failure when using the phenological monitoring station data for verification, or the accuracy will be greatly affected. Therefore, we needed to establish a buffer near the phenological monitoring station to improve the spatial resolution. Each phenological station was set up with a buffer zone of 3 km [49]. The average of all pixel estimates of winter wheat in the buffer zone represents the phenological date of phenological monitoring stations. In addition, due to the limited data of phenological monitoring stations, MCD12Q2 products were used to verify the extracted results of HD and predicted results of MD. Since MCD12Q2 is a phenological product extracted from vegetation, winter wheat distribution was used to mask MCD12Q2 product. At the same time, due to the rotation of winter wheat and corn in Hebei province, some cycle values were extracted incorrectly due to data quality problems in MCD12Q2 products, which led to the incorrect classification of corn phenology into winter wheat phenology. Specifically, the phenological data of MCD12Q2 were first extracted based on the distribution of winter wheat. Secondly, the “NumCycles” parameter corresponding to MCD12Q2 phenological phase data was obtained, which represents the number of cycles of vegetation extraction. If the “NumCycles” parameter value is 1, and the occurrence date of this phenological phase is much greater than that of the actual date of phenological phase of winter wheat (for example, the phenological phase date reaches October, and the winter wheat has been harvested in July at the latest), then these data

are considered abnormal data and need to be deleted. In this paper, we removed such abnormal data.

In this study, the coefficient of determination (R^2), root mean square error (RMSE), and Bias are used to assess the monitor and predictive performance [49]. R^2 reflects the consistency of the estimated and predicted results with the observed data and MCD12Q2 phenological products. The larger the value is, the higher the consistency; otherwise, the lower the value is, the worse the consistency. RMSE is the average deviation between the estimated and predicted results and the observed data and MCD12Q2 phenological products—the smaller the value, the higher the accuracy. Bias is the deviation between the estimated and predicted results and the observed data and MCD12Q2 phenological products. If the value is less than 0, the estimated and predicted results are earlier than the observed data and MCD12Q2. If the value is greater than 0, it indicates that the estimated and predicted results are later than the observed data and MCD12Q2. The smaller the absolute value of Bias, the higher the accuracy of the estimation result.

R^2 , RMSE, and Bias are defined as follows [35]:

$$R^2 = \frac{\sum_{i=1}^n (y_i' - \bar{y})^2}{\sum_{i=1}^n (y_i - \bar{y})^2} \quad (5)$$

$$RMSE = \sqrt{\frac{1}{n} \sum_{i=1}^n (y_i' - y_i)^2} \quad (6)$$

$$Bias = \frac{1}{n} \sum_{i=1}^n (y_i' - y_i) \quad (7)$$

where n represents the number of samples, y_i represents the observed value, y_i' represents the predicted value, and \bar{y} represents the average observed value.

4. Results

4.1. The Consistency of Ground Observed Data and MCD12Q2 Data

The MCD12Q2 product was created by assembling time series of NBAR-EVI2, eliminating outliers, and filling dormant period values; fitting a Quality assurance (QA)/Quality control (QC)-weighted penalized cubic smoothing spline to the time series; identifying valid vegetation cycles within the time series; and then extracting and recording phenometrics for each vegetation cycle.

In order to reveal the rationality of using the MCD12Q2 phenology product to verify the predicted MD, we compared the MD of the MCD12Q2 phenology product with the MD obtained by the ground phenology station (Figure 3). As shown in Figure 3, the MD of the MCD12Q2 phenology product is consistent with the maturity date obtained by the ground phenology station, and the R^2 reached 0.9. Bias is 1.29 days and RMSE is 2.59 days.

4.2. The Spatial Pattern of Estimated HD and Predicted MD

4.2.1. The Spatial Pattern of Estimated HD

The results of the HD of winter wheat in Hebei Province in 2018 extracted based on the maximum value method and phenological product MCD12Q2 extracted based on maximum method are shown in Figure 4. As can be seen from Figure 4, the HD distribution of winter wheat extracted by the two methods is consistent in general. From south to north, heading time gradually delayed with the increase in latitude. The HD extracted by the maximum method was earlier than that extracted by MCD12Q2, especially in the south. The HD extracted with MCD12Q2 was on 30 April (DOY110), about 10 days apart.

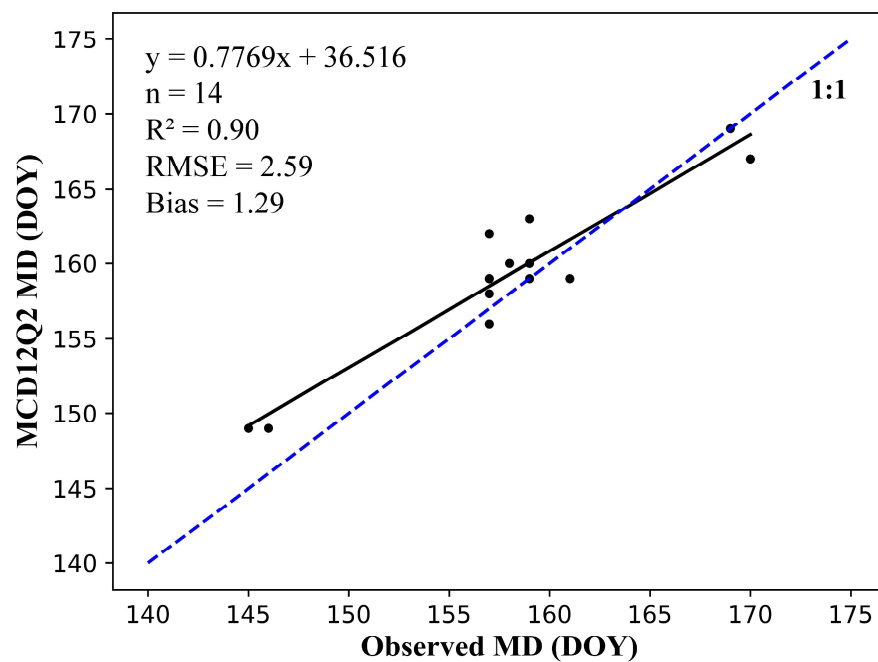


Figure 3. The consistency of ground observed data and MCD12Q2 data.

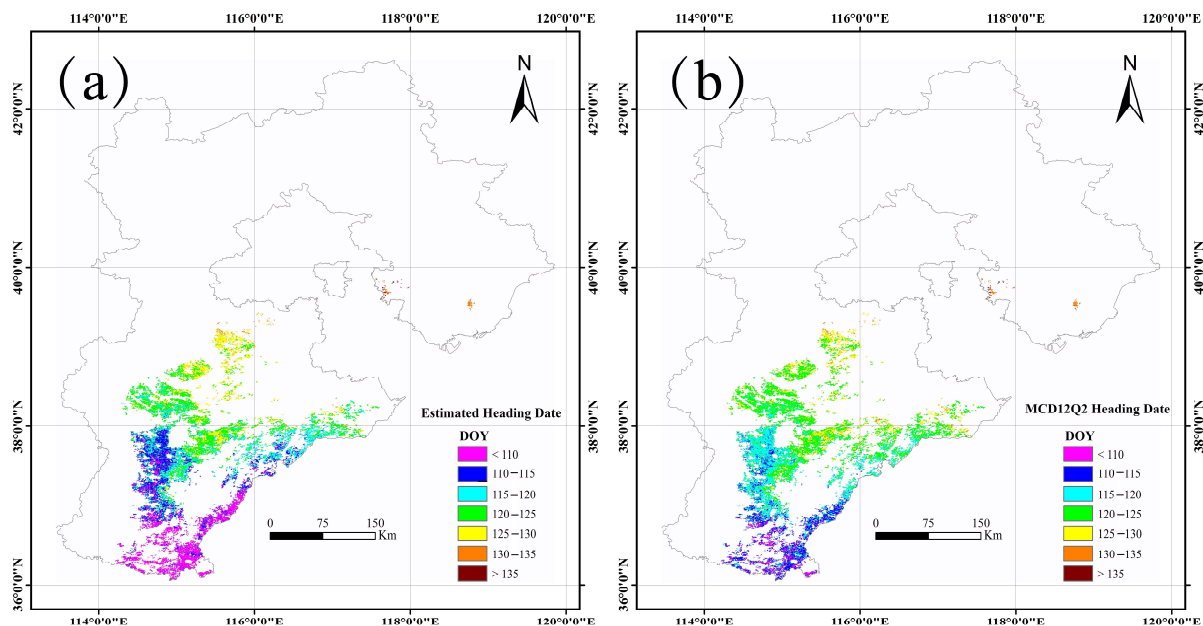


Figure 4. Spatial distribution of winter wheat HD by (a) estimation and (b) MCD12Q2 product.

4.2.2. The Spatial Pattern of Predicted MD

The results of the MD prediction of winter wheat in Hebei Province in 2018 based on the HD and accumulated effective temperature were compared with the results of the MD extracted from the phenological product MCD12Q2. As shown in Figure 5, the overall distribution of the MD of winter wheat extracted by the two methods is consistent, ranging from 23 May (DOY143) to 17 June (DOY168), with the MD gradually delayed from south to north. The earliest MD can be seen in Figure 5a, which is located in the southernmost part of the study area and enters the MD in late May; the latest MD is located in the northeastern part of the study area and enters MD in mid-June. By comparing Figure 5a,b, the predicted MD is earlier in south-central Hebei Province than that extracted from the MCD12Q2 product.

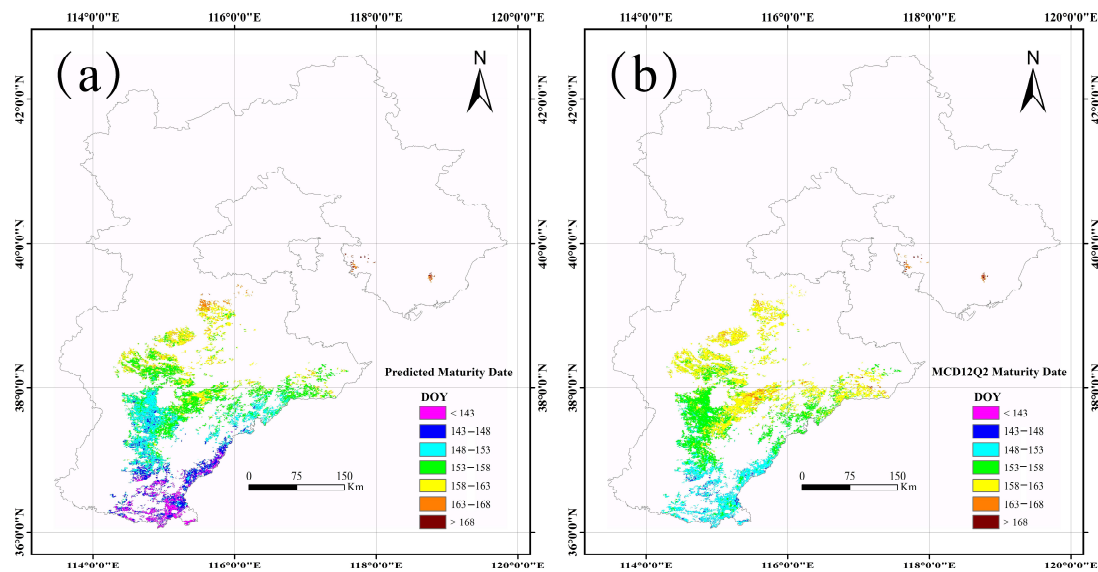


Figure 5. Spatial distribution of winter wheat MD by (a) prediction and (b) MCD12Q2 product.

4.3. Evaluation of HD Estimation Accuracy

As shown in Figure 6, the estimated HD of winter wheat was validated by ground observation data and MCD12Q2 data. Figure 6a shows the validation of the estimated HD using the observed HD from 14 phenological stations; R^2 is not very high, only 0.33; Bias is 3.93 days; and RMSE is 7.31 days.

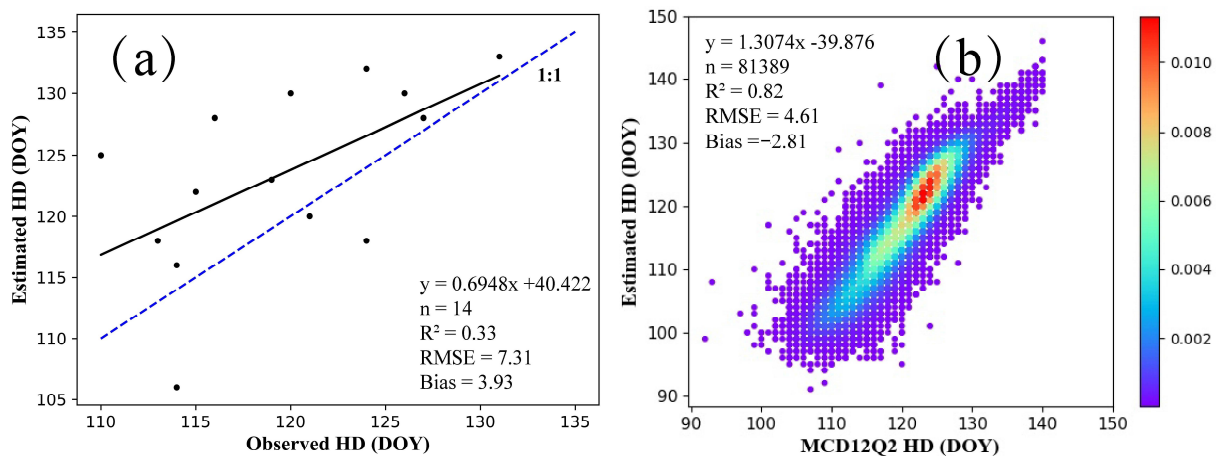


Figure 6. The validation of estimated HD of winter wheat by (a) ground observed data and (b) MCD12Q2 data.

To further evaluate the performance of the maximum value method to extract the HD, we validated the estimated HD using the HD extracted by the phenological product MCD12Q2, and we drew scatter plots of the HD obtained by the two methods for all winter wheat samples in Hebei Province. As shown in Figure 6b, the maximum method extracting the HD has good performance with R^2 reaching 0.82, Bias of -2.81 , and RMSE of 4.61 days.

4.4. Evaluation of MD Prediction Accuracy

The predicted MD of winter wheat was validated by ground observations and MCD12Q2 data, as shown in Figure 7. Figure 7a shows the validation of the MD predicted using the observed MD from 14 phenology stations; R^2 reached 0.48, Bias was 4.93 days, and RMSE was 7.03 days.

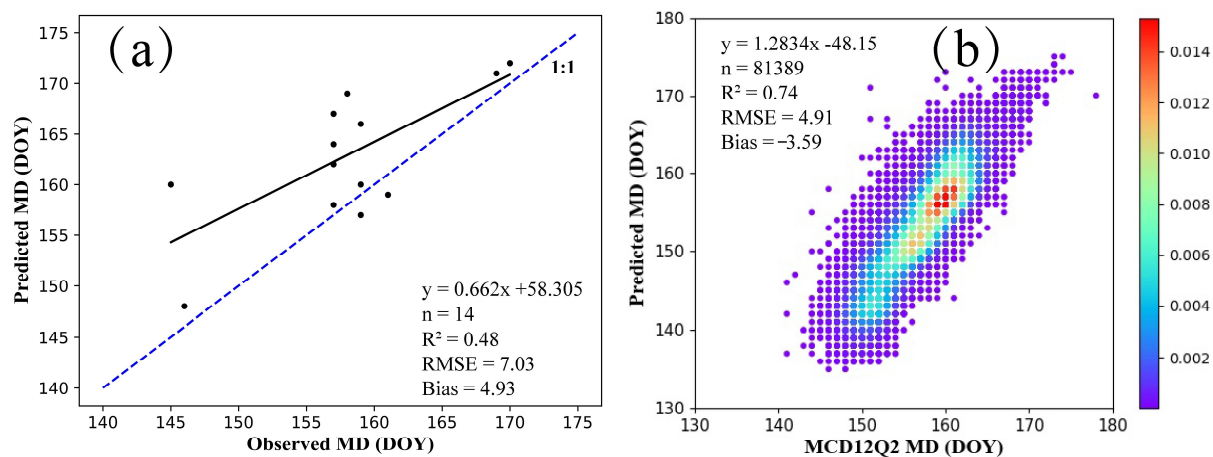


Figure 7. The validation of predicted MD of winter wheat by (a) ground observed data and (b) MCD12Q2 data.

To further evaluate the performance of the accumulated effective temperature extracted MD, we used the MD extracted by the phenology product MCD12Q2 to validate the estimated MD, and we plotted the MD scatter plots obtained by the two methods for all winter wheat samples in Hebei Province. As shown in Figure 7b, the MD extracted by the accumulated effective temperature method has good performance with R^2 reaching 0.74, Bias of -3.59 , and RMSE of 4.91 days.

5. Discussion

5.1. Advantages of the Proposed Method

At present, there are three methods to predict crop phenology, which are based on empirical models, crop models, and remote sensing data. However, these three methods have certain limitations for the prediction of crop phenology on a large regional scale. Firstly, the method based on empirical model is based on the statistical analysis of crop historical data. According to the empirical model, the law of crop growth and development is summarized, and this law is used to predict the phenological period of crops. The advantages of this method are simple and small driving parameters. However, this method also has obvious limitations. It ignores the impact of crop management factors, terrain, and climate factors on crop growth, which often exist at a large regional scale. This will make it difficult to replicate such methods on a large regional scale [50–52]. Secondly, the crop model describes the process of crop growth and development from the growth mechanism driven by crop photosynthesis. Using the growth model to build a cost function with crop yield as the optimization objective, it can be solved inversely, optimize the harvest time of crops, and realize the prediction of crop phenology. However, this method requires many parameters, such as sowing date, variety, and soil information, and the difficulty of calibrating crop growth model on a large regional scale limits its applications [30,53]. In addition, the prediction of phenological period based on remote sensing data has high requirements for the time and spatial resolution of remote sensing data. Due to the influence of cloud, rain, snow, and other factors, high-quality remote sensing images of the areas that need to be studied cannot be guaranteed in the key growth period of crops.

The method proposed in this study combines the spatial and temporal advantages of MODIS time series data and air temperature data and realizes the prediction of winter wheat maturity. Remote sensing data have the characteristics of wide coverage, multitemporal, spatial continuity, and so on. It can well-reflect the changes of crop growth on a large regional scale. Therefore, the crop can be monitored by remote sensing data, and the parameters required by the accumulated temperature model can be provided, such as sowing date, green returning period, and heading period. The air temperature data have a high time resolution. Using the air temperature data and historical phenological period data, the required accumulated temperature of crops from one phenological period to

another can be calculated accurately so as to build an effective accumulated temperature model. Using the phenological period obtained from remote sensing data as the starting point of accumulated temperature, combined with the accumulated temperature model and meteorological forecast data, it is easy to predict the crop phenological phase.

5.2. Limitations and Future Perspectives

The method in this paper also has some drawbacks. First, the calculation of cumulative temperature requires meteorological data, which have a lower spatial resolution compared with remote sensing data; this affects the accuracy of prediction when it is necessary to predict the phenological phases on a large scale. Secondly, when calculating the average cumulative temperature, the phenological observation data of historical years are needed, and sometimes such historical phenological observation data are limited. Next, this method is based on monitoring the previous phenological phases and predicting the next phenological phases from the accumulated temperature. The error of monitoring the previous phenological phases will be passed to the later phenological phases' prediction, which will lead to an increase in the phenological phases' prediction error. Finally, this method requires forecast temperature data to calculate the cumulative temperature. Although the accuracy of forecast temperature data has improved with the development of numerical prediction and assimilation techniques, there are still differences compared with the real temperature data. In addition, the forecast length and resolution need to be further improved, for example, the THORPEX Interactive Grand Global Ensemble (TIGGE) dataset only has a maximum 15-day forecast capability with a spatial resolution of 0.25 degrees [30], indicating that each pixel corresponds to 25 km by 25 km. The subseasonal to seasonal (S2S) forecast temperature data have a maximum 45-day forecast capability, but the spatial resolution is even lower at 1.5 degrees, indicating that each pixel corresponds to 150 km by 150 km.

Based on the abovementioned limitations, we plan to focus on the following aspects in our future research. In terms of data, firstly, since there is a relationship between temperature product data and ground temperature data, we can consider using meteorological data and ground temperature data to build a ground-meteorological conversion model, so as to replace the low-resolution meteorological data with ground temperature data with high spatial resolution and improve the prediction accuracy of the phenological phases. Secondly, for forecast data, we can try some medium- and long-term prediction capability and air-turning variable green higher regional climate models [54]. In terms of the method, if the phenological phases of historical years are missing, the spatially available data of the current year can be considered to solve the problem. In addition, direct prediction of remote sensing time series data can be considered to avoid the error transfer problem.

6. Conclusions

This paper proposes a method to predict the maturity date of winter wheat based on MODIS EVI2 remote sensing time series data and cumulative temperature. Firstly, the maximum value method is used to extract the heading date from MODIS EVI2 time series; secondly, the historical phenological data and meteorological data are combined to obtain the average cumulative temperature required from the heading date to the maturity date of winter wheat. Finally, the maturity date of winter wheat was predicted by combining the heading date and the current year's cumulative temperature. The conclusions of the study are as follows: (1) MCD12Q2, as a vegetation phenological product, has a high maturity agreement with the maturity of ground winter wheat phenological observation stations, with R^2 reaching 0.9, and RMSE and Bias of 2.59 and 1.29 days, respectively. Therefore, the MCD12Q2 vegetation phenological product can be used for result validation. (2) The accuracy of the method in predicting maturity was high in this paper, which was validated by the data from the ground phenological observation stations and MCD12Q2 vegetation phenological product, and the results showed that the R^2 for predicting MD using this method was 0.48 and 0.74, RMSE was 7.03 and 4.91 days, and Bias was 4.93 and -3.59 days,

respectively. This method can accurately predict the phenological phase of winter wheat at the regional scale.

Author Contributions: Conceptualization, F.Z. and G.Y.; methodology, G.Y., H.Y. and F.Z.; data curation, F.Z., Y.Z. and S.H.; formal analysis, F.Z., W.X., Y.M. and M.L.; writing—original draft preparation, F.Z.; writing—review and editing, G.Y., H.L. and H.Y. All authors have read and agreed to the published version of the manuscript.

Funding: This research was funded by the Natural Science Foundation of China (42171303), the National Key Research and Development Program of China (2019YFE0125300, 2017YFE0122500), and the Special Fund for Construction of Scientific and Technological Innovation Ability of Beijing Academy of Agriculture and Forestry Sciences (KJCX20210433) and Chongqing Technology Innovation and Application Development Special Project (cstc2019jscx-gksbX0092, cstc2021jscx-gksbX0064).

Institutional Review Board Statement: Not applicable.

Informed Consent Statement: Not applicable.

Data Availability Statement: The remote sensing data, MCD12Q2 product data and meteorological data were downloaded through the Google Earth Engine (GEE) platform (<https://earthengine.google.com>, accessed on 20 October 2021). The phenological monitoring station data were obtained from the meteorological data sharing service system of China (<http://data.cma.cn>, accessed on 10 October 2021).

Acknowledgments: We would like to thank our collaborators from the Key Laboratory of Quantitative Remote Sensing in Agriculture of Ministry of Agriculture and Rural Affairs, National Engineering Research Center for Information Technology in Agriculture, Chang'an University and Anhui University. We also thank the anonymous reviewers and the academic editor for their valuable comments and recommendations.

Conflicts of Interest: The authors declare no conflict of interest.

References

1. Cisternas, I.; Velásquez, I.; Caro, A.; Rodríguez, A. Systematic literature review of implementations of precision agriculture. *Comput. Electron. Agric.* **2020**, *176*, 105626. [\[CrossRef\]](#)
2. Yost, M.A.; Kitchen, N.R.; Sudduth, K.A.; Sadler, E.J.; Drummond, S.T.; Volkmann, M.R. Long-term impact of a precision agriculture system on grain crop production. *Precis. Agric.* **2017**, *18*, 823–842. [\[CrossRef\]](#)
3. Pathak, H.S.; Brown, P.; Best, T. A systematic literature review of the factors affecting the precision agriculture adoption process. *Precis. Agric.* **2019**, *20*, 1292–1316. [\[CrossRef\]](#)
4. Atkinson, P.M.; Jeganathan, C.; Dash, J.; Atzberger, C. Inter-comparison of four models for smoothing satellite sensor time-series data to estimate vegetation phenology. *Remote Sens. Environ.* **2012**, *123*, 400–417. [\[CrossRef\]](#)
5. Verhegghen, A.; Bontemps, S.; Defourny, P. A global NDVI and EVI reference data set for land-surface phenology using 13 years of daily SPOT-VEGETATION observations. *Int. J. Remote Sens.* **2014**, *35*, 2440–2471. [\[CrossRef\]](#)
6. Yu, L.X.; Liu, T.X.; Bu, K.; Yan, F.Q.; Yang, J.C.; Chang, L.P.; Zhang, S.W. Monitoring the long term vegetation phenology change in Northeast China from 1982 to 2015. *Sci. Rep.* **2017**, *7*, 14770. [\[CrossRef\]](#)
7. Sakamoto, T.; Wardlow, B.D.; Gitelson, A.A.; Verma, S.B.; Suyker, A.E.; Arkebauer, T.J. A Two-Step Filtering approach for detecting maize and soybean phenology with time-series MODIS data. *Remote Sens. Environ.* **2010**, *114*, 2146–2159. [\[CrossRef\]](#)
8. Sakamoto, T.; Gitelson, A.A.; Arkebauer, T.J. MODIS-based corn grain yield estimation model incorporating crop phenology information. *Remote Sens. Environ.* **2013**, *131*, 215–231. [\[CrossRef\]](#)
9. Zeng, L.L.; Wardlow, B.D.; Xiang, D.X.; Hu, S.; Li, D.R. A review of vegetation phenological metrics extraction using time-series, multispectral satellite data. *Remote Sens. Environ.* **2020**, *237*, 111511. [\[CrossRef\]](#)
10. Chen, J.; Rao, Y.H.; Shen, M.G.; Wang, C.; Zhou, Y.; Ma, L.; Tang, Y.H.; Yang, X. A Simple Method for Detecting Phenological Change from Time Series of Vegetation Index. *IEEE Trans. Geosci. Remote Sens.* **2016**, *54*, 3436–3449. [\[CrossRef\]](#)
11. Vrieling, A.; de Leeuw, J.; Said, M.Y. Length of Growing Period over Africa: Variability and Trends from 30 Years of NDVI Time Series. *Remote Sens.* **2013**, *5*, 982–1000. [\[CrossRef\]](#)
12. Vrieling, A.; Meroni, M.; Darvishzadeh, R.; Skidmore, A.K.; Wang, T.J.; Zurita-Milla, R.; Oosterbeek, K.; O'Connor, B.; Paganini, M. Vegetation phenology from Sentinel-2 and field cameras for a Dutch barrier island. *Remote Sens. Environ.* **2018**, *215*, 517–529. [\[CrossRef\]](#)
13. Jönsson, P.; Cai, Z.Z.; Melaas, E.; Friedl, M.A.; Eklundh, L. A Method for Robust Estimation of Vegetation Seasonality from Landsat and Sentinel-2 Time Series Data. *Remote Sens.* **2018**, *10*, 635. [\[CrossRef\]](#)

14. Li, J.; Roy, D.P. A Global Analysis of Sentinel-2A, Sentinel-2B and Landsat-8 Data Revisit Intervals and Implications for Terrestrial Monitoring. *Remote Sens.* **2017**, *9*, 902. [\[CrossRef\]](#)
15. Zhou, Q.; Rover, J.; Brown, J.; Worstell, B.; Howard, D.; Wu, Z.T.; Gallant, A.L.; Rundquist, B.; Burke, M. Monitoring Landscape Dynamics in Central U.S. Grasslands with Harmonized Landsat-8 and Sentinel-2 Time Series Data. *Remote Sens.* **2019**, *11*, 328. [\[CrossRef\]](#)
16. Liu, L.L.; Zhang, X.Y.; Yu, Y.Y.; Guo, W. Real-time and short-term predictions of spring phenology in North America from VIIRS data. *Remote Sens. Environ.* **2017**, *194*, 89–99. [\[CrossRef\]](#)
17. Zhang, X.Y.; Jayavelu, S.; Liu, L.L.; Friedl, M.A.; Henebry, G.M.; Liu, Y.; Schaaf, C.B.; Richardson, A.D.; Gray, J. Evaluation of land surface phenology from VIIRS data using time series of PhenoCam imagery. *Agric. For. Meteorol.* **2018**, *256–257*, 137–149. [\[CrossRef\]](#)
18. Guyon, D.; Guillot, M.; Vitasse, Y.; Cardot, H.; Hagolle, O.; Delzon, S.; Wigneron, J.-P. Monitoring elevation variations in leaf phenology of deciduous broadleaf forests from SPOT/VEGETATION time-series. *Remote Sens. Environ.* **2011**, *115*, 615–627. [\[CrossRef\]](#)
19. Zheng, Y.; Wu, B.F.; Zhang, M.; Zeng, H.W. Crop Phenology Detection Using High Spatio-Temporal Resolution Data Fused from SPOT5 and MODIS Products. *Sensors* **2016**, *16*, 2099. [\[CrossRef\]](#)
20. White, M.A.; Thornton, P.E.; Running, S.W. A continental phenology model for monitoring vegetation responses to interannual climatic variability. *Glob. Biogeochem. Cycles* **1997**, *11*, 217–234. [\[CrossRef\]](#)
21. Jönsson, P.; Eklundh, L. TIMESAT—A program for analyzing time-series of satellite sensor data. *Comput. Geosci.* **2004**, *30*, 833–845. [\[CrossRef\]](#)
22. Vrieling, A.; Skidmore, A.K.; Wang, T.; Meroni, M.; Ens, B.J.; Oosterbeek, K.; O'Connor, B.; Darvishzadeh, R.; Heurich, M.; Shepherd, A.; et al. Spatially detailed retrievals of spring phenology from single-season high-resolution image time series. *Int. J. Appl. Earth Obs. Geoinf.* **2017**, *59*, 19–30. [\[CrossRef\]](#)
23. Gan, L.Q.; Cao, X.; Chen, X.H.; Dong, Q.; Cui, X.H.; Chen, J. Comparison of MODIS-based vegetation indices and methods for winter wheat green-up date detection in Huanghuai region of China. *Agric. For. Meteorol.* **2020**, *288–289*, 108019. [\[CrossRef\]](#)
24. Zhang, X.Y.; Friedl, M.A.; Schaaf, C.B.; Strahler, A.H.; Hodges, J.C.F.; Gao, F.; Reed, B.C.; Huete, A. Monitoring vegetation phenology using MODIS. *Remote Sens. Environ.* **2003**, *84*, 471–475. [\[CrossRef\]](#)
25. Sakamoto, T.; Yokozawa, M.; Toritani, H.; Shibayama, M.; Ishitsuka, N.; Ohno, H. A crop phenology detection method using time-series MODIS data. *Remote Sens. Environ.* **2005**, *96*, 366–374. [\[CrossRef\]](#)
26. Lu, L.L.; Wang, C.Z.; Guo, H.D.; Li, Q.T. Detecting winter wheat phenology with SPOT-VEGETATION data in the North China Plain. *Geocarto Int.* **2014**, *29*, 244–255. [\[CrossRef\]](#)
27. Liu, Z.J.; Wu, C.Y.; Liu, Y.S.; Wang, X.Y.; Fang, B.; Yuan, W.P.; Ge, Q.S. Spring green-up date derived from GIMMS3g and SPOT-VGT NDVI of winter wheat cropland in the North China Plain. *ISPRS J. Photogramm.* **2017**, *130*, 81–91. [\[CrossRef\]](#)
28. Chu, L.; Liu, Q.-S.; Huang, C.; Liu, G.-H. Monitoring of winter wheat distribution and phenological phases based on MODIS time-series: A case study in the Yellow River Delta, China. *J. Integr. Agric.* **2016**, *15*, 2403–2416. [\[CrossRef\]](#)
29. Chu, L.; Huang, C.; Liu, Q.-S.; Liu, G.-H. Estimation of winter wheat phenology under the influence of cumulative temperature and soil salinity in the Yellow River Delta, China, using MODIS time-series data. *Int. J. Remote Sens.* **2016**, *37*, 2211–2232. [\[CrossRef\]](#)
30. Zhuo, W.; Huang, J.X.; Gao, X.R.; Ma, H.Y.; Huang, H.; Su, W.; Meng, J.H.; Li, Y.; Chen, H.L.; Yin, D.Q. Prediction of Winter Wheat Maturity Dates through Assimilating Remotely Sensed Leaf Area Index into Crop Growth Model. *Remote Sens.* **2020**, *12*, 2896. [\[CrossRef\]](#)
31. Burke, M.W.V.; Rundquist, B.C. Scaling Phenocam GCC, NDVI, and EVI2 with Harmonized Landsat-Sentinel using Gaussian Processes. *Agric. For. Meteorol.* **2021**, *300*, 108316. [\[CrossRef\]](#)
32. Xu, X.M.; Conrad, C.; Doktor, D. Optimising Phenological Metrics Extraction for Different Crop Types in Germany Using the Moderate Resolution Imaging Spectrometer (MODIS). *Remote Sens.* **2017**, *9*, 254. [\[CrossRef\]](#)
33. Song, Y.; Wang, J.; Yu, Q.; Huang, J. Using MODIS LAI Data to Monitor Spatio-Temporal Changes of Winter Wheat Phenology in Response to Climate Warming. *Remote Sens.* **2020**, *12*, 786. [\[CrossRef\]](#)
34. Liang, W.-L.; Carberry, P.; Wang, G.-Y.; Lü, R.-H.; Lü, H.-Z.; Xia, A.-P. Quantifying the yield gap in wheat–maize cropping systems of the Hebei Plain, China. *Field Crop. Res.* **2011**, *124*, 180–185. [\[CrossRef\]](#)
35. Zhao, F.; Yang, G.J.; Yang, X.D.; Cen, H.Y.; Zhu, Y.H.; Han, S.Y.; Yang, H.; He, Y.; Zhao, C.J. Determination of Key Phenological Phases of Winter Wheat Based on the Time-Weighted Dynamic Time Warping Algorithm and MODIS Time-Series Data. *Remote Sens.* **2021**, *13*, 1836. [\[CrossRef\]](#)
36. Maus, V.; Camara, G.; Cartaxo, R.; Sanchez, A.; Ramos, F.M.; de Queiroz, G.R. A Time-Weighted Dynamic Time Warping Method for Land-Use and Land-Cover Mapping. *IEEE J. Sel. Top. Appl. Earth Obs. Remote Sens.* **2016**, *9*, 3729–3739. [\[CrossRef\]](#)
37. Belgiu, M.; Csillik, O. Sentinel-2 cropland mapping using pixel-based and object-based time-weighted dynamic time warping analysis. *Remote Sens. Environ.* **2018**, *204*, 509–523. [\[CrossRef\]](#)
38. Cheng, K.; Wang, J. Forest-Type Classification Using Time-Weighted Dynamic Time Warping Analysis in Mountain Areas: A Case Study in Southern China. *Forests* **2019**, *10*, 1040. [\[CrossRef\]](#)

39. Chaves, M.E.D.; Alves, M.D.C.; Sáfadi, T.; de Oliveira, M.S.; Picoli, M.C.A.; Simoes, R.E.O.; Mataveli, G.A.V. Time-weighted dynamic time warping analysis for mapping interannual cropping practices changes in large-scale agro-industrial farms in Brazilian Cerrado. *Sci. Remote Sens.* **2021**, *3*, 100021. [\[CrossRef\]](#)
40. Gorelick, N.; Hancher, M.; Dixon, M.; Ilyushchenko, S.; Thau, D.; Moore, R. Google Earth Engine: Planetary-scale geospatial analysis for everyone. *Remote Sens. Environ.* **2017**, *202*, 18–27. [\[CrossRef\]](#)
41. Qiu, T.; Song, C.; Clark, J.S.; Seyednasrollah, B.; Rathnayaka, N.; Li, J. Understanding the continuous phenological development at daily time step with a Bayesian hierarchical space-time model: Impacts of climate change and extreme weather events. *Remote Sens. Environ.* **2020**, *247*, 111956. [\[CrossRef\]](#)
42. Zhang, X.; Liu, L.; Liu, Y.; Senthilnath, J.; Schaaf, C.B. Generation and evaluation of the VIIRS land surface phenology product. *Remote Sens. Environ.* **2018**, *216*, 212–229. [\[CrossRef\]](#)
43. Xiao, W.; Sun, Z.; Wang, Q.; Yang, Y. Evaluating MODIS phenology product for rotating croplands through ground observations. *J. Appl. Remote Sens.* **2013**, *7*, 073562. [\[CrossRef\]](#)
44. Duan, T.; Chapman, S.C.; Guo, Y.; Zheng, B. Dynamic monitoring of NDVI in wheat agronomy and breeding trials using an unmanned aerial vehicle. *Field Crop. Res.* **2017**, *210*, 71–80. [\[CrossRef\]](#)
45. Zheng, H.B.; Cheng, T.; Yao, X.; Deng, X.Q.; Tian, Y.C.; Cao, W.X.; Zhu, Y. Detection of rice phenology through time series analysis of ground-based spectral index data. *Field Crop. Res.* **2016**, *198*, 131–139. [\[CrossRef\]](#)
46. Jeong, S.-J.; Ho, C.-H.; Gim, H.-J.; Brown, M.E. Phenology shifts at start vs. end of growing season in temperate vegetation over the Northern Hemisphere for the period 1982–2008. *Glob. Chang. Biol.* **2011**, *17*, 2385–2399. [\[CrossRef\]](#)
47. Piao, S.L.; Fang, J.Y.; Zhou, L.M.; Ciais, P.; Zhu, B. Variations in satellite-derived phenology in China's temperate vegetation. *Glob. Chang. Biol.* **2006**, *12*, 672–685. [\[CrossRef\]](#)
48. Cong, N.; Piao, S.L.; Chen, A.P.; Wang, X.H.; Lin, X.; Chen, S.P.; Han, S.J.; Zhou, G.S.; Zhang, X.P. Spring vegetation green-up date in China inferred from SPOT NDVI data: A multiple model analysis. *Agric. For. Meteorol.* **2012**, *165*, 104–113. [\[CrossRef\]](#)
49. Huang, X.; Zhu, W.Q.; Wang, X.Y.; Zhan, P.; Liu, Q.F.; Li, X.Y.; Sun, L.X. A Method for Monitoring and Forecasting the Heading and Flowering Dates of Winter Wheat Combining Satellite-Derived Green-Up Dates and Accumulated Temperature. *Remote Sens.* **2020**, *12*, 3536. [\[CrossRef\]](#)
50. Jingjing, X.; Quan, L.; Ganghua, L.; Yonglin, D.; Zhao, Z.; Wang, S.; Ding, Y. The study of spatial and temporal characteristics of safe maturity dates of rice in Jiangsu Province. *J. Nanjing Agric. Univ.* **2013**, *36*, 1–6.
51. Gong, J.L.; Xing, Z.P.; Ya-Jie, H.U.; Zhang, H.C.; Dai, Q.G.; Huo, Z.Y.; Ke, X.U.; Wei, H.Y.; Gao, H. Difference in Growth Duration and Utilization of Temperature and Solar Radiation Between indica and japonica Super Rice in the Lower Yangtze and Huaihe River Valley. *Chin. J. Rice Sci.* **2014**, *28*, 267–276.
52. Wu, J.J.; Wang, Y.; Shen, H.Z.; Wang, Y.Q.; Ma, X.Y. Evaluating the accuracy of ARMA and multi-index methods for predicting winter wheat maturity date. *J. Sci. Food Agric.* **2021**, *102*, 2484–2493. [\[CrossRef\]](#) [\[PubMed\]](#)
53. Huang, J.; Tian, L.; Liang, S.; Ma, H.; Becker-Reshef, I.; Huang, Y.; Su, W.; Zhang, X.; Zhu, D.; Wu, W. Improving winter wheat yield estimation by assimilation of the leaf area index from Landsat TM and MODIS data into the WOFOST model. *Agric. For. Meteorol.* **2015**, *204*, 106–121. [\[CrossRef\]](#)
54. Lv, Z.F.; Liu, X.J.; Cao, W.X.; Zhu, Y. Climate change impacts on regional winter wheat production in main wheat production regions of China. *Agric. For. Meteorol.* **2013**, *171–172*, 234–248. [\[CrossRef\]](#)